High Li+ and Mg2+ Conductivity in a Cu-Azolate Metal–Organic Framework

High Li^+ and Mg^{2+} conductivity in a Cu-azolate metal-organic framework

Elise M. Miner, Sarah S. Park, and Mircea Dincă*

Department of Chemistry, Massachusetts Institute of Technology, 77 Massachusetts Avenue, Cambridge, Massachusetts 02139, United States

Supporting Information

ABSTRACT: A Cu-azolate metal-organic framework uptakes stoichiometric loadings of Group 1 and 2 metal halides, demonstrating efficient reversible release and reincorporation of immobilized anions within the framework. Ion pairing interactions lead to anion-dependent Li^+ and Mg^{2+} transport in $Cu_4(ttpm)_2 \cdot 0.6CuCl_2$, whose high surface area affords a high density of uniformly distributed mobile metal cations and halide binding sites. The ability to systematically tune the ionic conductivity yields a solid electrolyte with a Mg^{2+} ion conductivity rivaling the best materials reported to date. This MOF is one of the first in a promising class of frameworks that introduces the opportunity to control the identity, geometry, and distribution of the cation hopping sites, offering a versatile template for application-directed design of solid electrolytes.

INTRODUCTION

Since the emergence of the first rechargeable galvanic cell in 1860,[1] rechargeable batteries have become an enabling technology for a range of critical processes in modern life. Although old in a sense, rechargeable battery technologies represent an important field of modern research, spurred by the scale and variety of applications stemming from an inevitable transition to renewable and clean energy technologies. Among the various possible technologies, metal and metal-ion batteries are particularly versatile in serving a range of applications especially in consumer electronics, where they offer a combination of high volumetric capacity and ~1000-cycle lifetime that is well suited for such devices.[2] However, despite significant advances there is much room for improvement in efficiency, lifetime, and safety of metal and metal-ion batteries. All these could be improved by transitioning from liquid electrolytes, the current industry standard, to solid ion conductors. Liquid electrolytes exhibit relatively narrow potential stability windows, cation transference numbers of < 0.4 that lead to lifetime-limiting polarization effects, and little control over the uniformity of Li plating during charging.[2] Non-uniform plating can cause dendrite formation, which may result in piercing the battery separator and leakage of the flammable organic liquid electrolyte, or if contact is made with the other electrode, circuit shorting. Efforts to address these challenges have included development of solid-state electrolytes.[3–17] Although solid electrolytes exhibit higher potential stability windows, higher transference numbers, and are safer by virtue of their reduced flammability and increased mechanical stability, they can suffer from low conductivity and poor interfacial contact between the electrodes and the electrolyte.[2–4,7,8] An ideal system would combine the lower transport and interfacial resistance of liquid electrolytes with the safety and enhanced stability features of solid electrolytes.

One class of materials that may provide clues to addressing these challenges is metal-organic frameworks (MOFs). The high surface area of MOFs offers the ability to install a high density of charged species in a small geometric volume. This allows for closely packed cation hopping sites, which could minimize activation energy for ion transport and increase ion conductivity. Additionally, the ordered porosity of MOFs could aid in controlling the uniformity of cation plating at the anode during charging, thus preventing dendrite formation. Many MOFs present metal sites whose coordination spheres are initially occupied by solvent molecules. Removing the solvent molecules exposes coordinatively unsaturated cationic sites onto which anions can be docked. The coordinated anions require charge-balancing cations that become the only mobile charge carriers, thus maximizing cation transference numbers. Finally, altering the lability and / or valency of the metal centers, changing pore polarity by ligand functionalization, and enlarging the pore diameter by extending the ligand length offer multiple tunable variables for systematic optimization of electrolyte performance. Indeed, several MOFs have been explored as solid-state electrolytes, and have featured many of the benefits listed above.[18–23] Although promising, many of these MOFs require additional salt content in excess of what would be expected based on the number of available anion binding sites. This necessarily implies that not only cations, but also anions will be mobile, which in turn reduces the cation transference numbers. Additionally, activation energies in such materials are sometimes higher than is desired, as ion pairing between anions and cations is still strong. Some of the reported MOF-based electrolytes have also shown poor stability to electrochemical cycling, eliminating their viability for rechargeable batteries. To expand upon current MOF electrolytes, we took advantage of a Cu-azolate material, $Cu_4(ttpm)_2$ (H_4ttpm = tetrakis(4-tetrazolylphenyl)methane)[24]

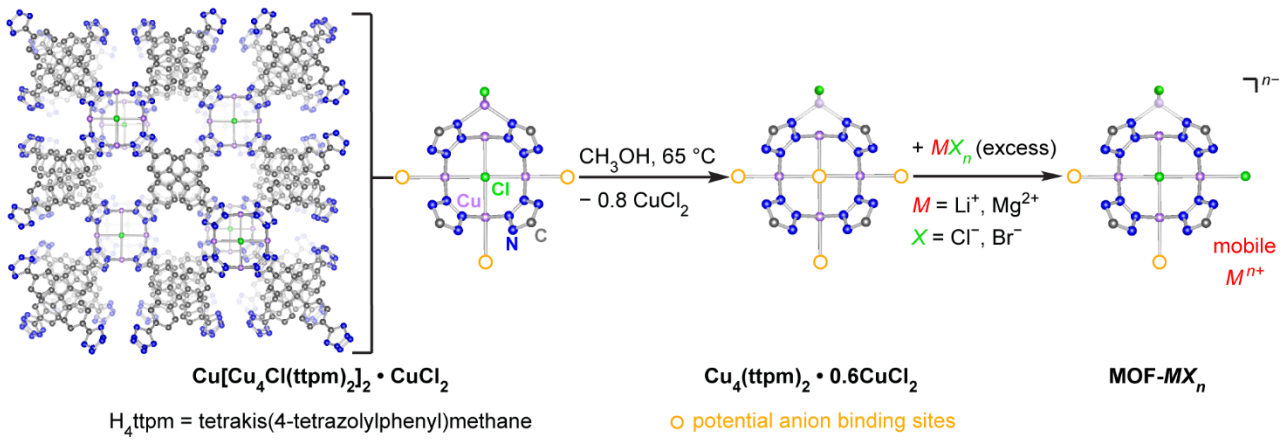

Scheme 1. Synthesis of $Cu[(Cu_4Cl)(ttpm)_2]_2{\cdot}CuCl_2$, $Cu_4(ttpm)_2{\cdot}0.6CuCl_2$, and the target MOF-$MX_n$, where M = Li^+ or Mg^{2+}, X = Cl^- or Br^-, and n = 1 or 2. H atoms have been omitted for clarity.

Table 1. Formulas of MOF-MX_n, including metal ratios as determined by ICP-MS and propylene carbonate (PC) content from ^{1}H NMR spectroscopy. Refer to Table S1 for weight percentages of M^{n+} in the electrolytes.

Sample name	Cu	M^{n+} (M^{n+} = Li^+, Mg^{2+})	X (X = Cl^-, Br^-, I^-)	Formula
MOF-LiCl	2.5	1.0	1.0	$Cu_4(ttpm)_2(CuCl_2)_{0.6}(LiCl)_{1.8}{\cdot}19PC$
MOF-LiBr	2.4	1.0	1.0	$Cu_4(ttpm)_2(CuCl_2)_{0.6}(LiBr)_{1.8}{\cdot}20PC$
MOF-LiI	4.5	1.0	1.0	$Cu_4(ttpm)_2(CuCl_2)_{0.6}(LiI)_{1.0}{\cdot}20PC$
MOF-$MgCl_2$	6.1	1.0	2.0	$Cu_4(ttpm)_2(CuCl_2)_{0.6}(MgCl_2)_{0.8}{\cdot}17PC$
MOF-$MgBr_2$	6.4	1.0	2.0	$Cu_4(ttpm)_2(CuCl_2)_{0.6}(MgBr_2)_{0.7}{\cdot}21PC$
MOF-MgI_2	7	1.0	2.0	$Cu_4(ttpm)_2(CuCl_2)_{0.6}(MgI_2)_{0.7}{\cdot}15PC$

that presents multiple anion binding sites, a key feature that enabled ionic conductivity in another MOF electrolyte previously reported by our group.[18] This abundance of anionic binding sites in $Cu_4(ttpm)_2$ leads to high mobile Li^+, Mg^{2+}, and Al^{3+} density. The ability to reconstitute this MOF in various types of metal salts allowed for modulation of the ion pairing strength, as evidenced by conductivity and activation energy values that change as a function of anion identity.

EXPERIMENTAL METHODS

Complete experimental methods are provided as Supporting Information.

RESULTS AND DISCUSSION

Preparation of MOF-MX_n. The anionic parent material, $Cu[(Cu_4Cl)(ttpm)_2]_2{\cdot}CuCl_2$, and the neutral framework, $Cu_4(ttpm)_2{\cdot}0.6CuCl_2$, were synthesized according to a reported procedure.[24] It was previously shown that Cu_4(tetrazole)$_8$ secondary building units (SBUs) in the original material feature 5 possible halide binding sites, a portion of which can be made available for anion binding by Soxhlet extraction with methanol (Scheme 1).[24] Importantly, some of these sites bear bridging halides, which opens the possibility of reducing their ion pairing with mobile cations because electron density on the bridging halides would be screened by multiple Cu^{2+} ions. Reconstitution of $Cu_4(ttpm)_2{\cdot}0.6CuCl_2$ in saturated THF solutions of various Group 1 and 2 metal halide salts (i.e. LiCl, LiBr, $MgCl_2$, $MgBr_2$) afforded anionic structures balanced with alkali and alkaline earth metal cations (Scheme 1). The resulting materials were washed with propylene carbonate (PC), a commonly used dielectric that solvates the metal cations and can improve inter-particle conductivity.[18,21] Inductively-coupled plasma-mass spectrometry (ICP-MS) and quantitative ^{1}H NMR spectroscopy of digested samples (Figures S1-S6) provided the Group 1 and 2 metal content and propylene carbonate content, respectively, for the final electrolyte formulations (Table 1). Soaking the MOF in solutions of LiCl, LiBr, $MgCl_2$, or $MgBr_2$ installed approximately 2 equivalents of halide per Cu_4 SBU. Stoichiometric reincorporation of immobilized anions promoted by appropriate equivalents of open metal sites within the host provides the potential to maximize cation transference numbers and modulate the ionic transport properties of the electrolyte by altering the identity of the immobilized anion.

That the coordination mode of the halides can be defined within the crystallographic parameters of the MOF as opposed to random dispersion of the salts within the electrolyte matrix was evidenced by powder X-ray diffraction (PXRD) and scanning electron microscopy-energy dispersive X-ray spectroscopy (SEM-EDS). Soxhlet-extracting the anionic

$Cu[(Cu_4Cl)(ttpm)_2]_2{\cdot}CuCl_2$ resulted in almost total disappearance of the [110] reflection at $2\theta \cong 8°$, which has electron density from both axial Cl^- and bridging μ_4-Cl^- as major contributors (Figure S7). PXRD patterns of the MOF-MX_n samples showed a reemergence of this reflection, consistent with immobilized halides having a crystallographically distinct coordination mode within the Cu_4 SBU (Figure 1, Figure S8).

PXRD also confirmed that the MOF retains its structure both during the treatment with halide salts, and during electrochemical cycling. However, treating the MOF with LiI or MgI_2 resulted in major reduction of crystallinity with the former and total destruction of the MOF structure with the latter (Figure S8). This is not unexpected, as I^- is readily oxidized by Cu^{2+} and CuI_2 itself is unstable to disproportionation.[25–28] In line with redox activity at the MOF Cu^{2+} sites, iodide-treated samples exhibit faradaic events that are not observed with the other halides (Figure S9).

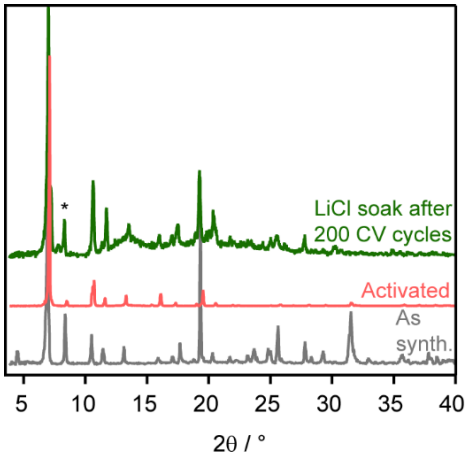

Figure 1. Representative PXRD pattern showcasing the disappearance and reemergence of the [110] reflection at $2\theta \cong 8°$ (largely contributed by the halide electron density), as well as stability of the MOF to electrochemical cycling. See Supplementary Figure S8 for PXRD patterns of the other analogues.

Further evidence for homogeneous incorporation of halides in the MOF-MXn electrolytes came from SEM-EDS (Figure S10). The homogeneity of chloride as well as copper distribution in the spectra confirmed that no amorphous MX_n phase had aggregated within the electrolyte matrix. Additionally, reduction of the average crystallite size by approximately two orders of magnitude during the halide soak was consistent with the MX_n salts penetrating the crystals themselves rather than residing in grain boundaries or other more kinetically accessible locations (Figure S10).

Conductivity measurements with MOF-MX_n. To ensure that the parent $Cu_4(ttpm)_2{\cdot}0.6CuCl_2$ was sufficiently electrically insulating to prevent short-circuiting, a 100 V potential (from –50 V to 50 V) was applied to a pressed pellet and the resulting current was measured. The generated I-V curve yielded an electrical conductivity of $5.08{\cdot}10^{-12}$ S·cm^{-1}, confirming that $Cu_4(ttpm)_2{\cdot}0.6CuCl_2$ is an electrical insulator and a suitable host as a solid electrolyte (Figure S11).[29]

To measure ionic conductivity, MOF-MX_n powders were loaded into a test cell and subjected to electrochemical impedance spectroscopy (EIS) from 1 MHz to 1 Hz. Fitting the resulting EIS spectra to the circuit shown in the Methods section (see Supporting Information) gave Li^+ conductivities ranging from $2.4{\cdot}10^{-5}$ S·cm^{-1} (MOF-LiCl) to $1.1{\cdot}10^{-4}$ (MOF-LiI) at 25 °C for the MOF-Li*X* samples (Figure 2, Table 2). Excitingly, this data highlighted the ability to systematically tune the conductivity by modulating the softness of the anion, in turn altering the ionic strength of the Li-halide interaction. Additional utility of this modular structure was showcased in the activation energies. Variable-temperature EIS (Figure S12) and fitting the corresponding Arrhenius plots gave activation energies which also varied as a function of anion softness (E_a = 0.34 eV for MOF-LiCl to 0.24 eV for MOF-LiI) (Table 2). These low

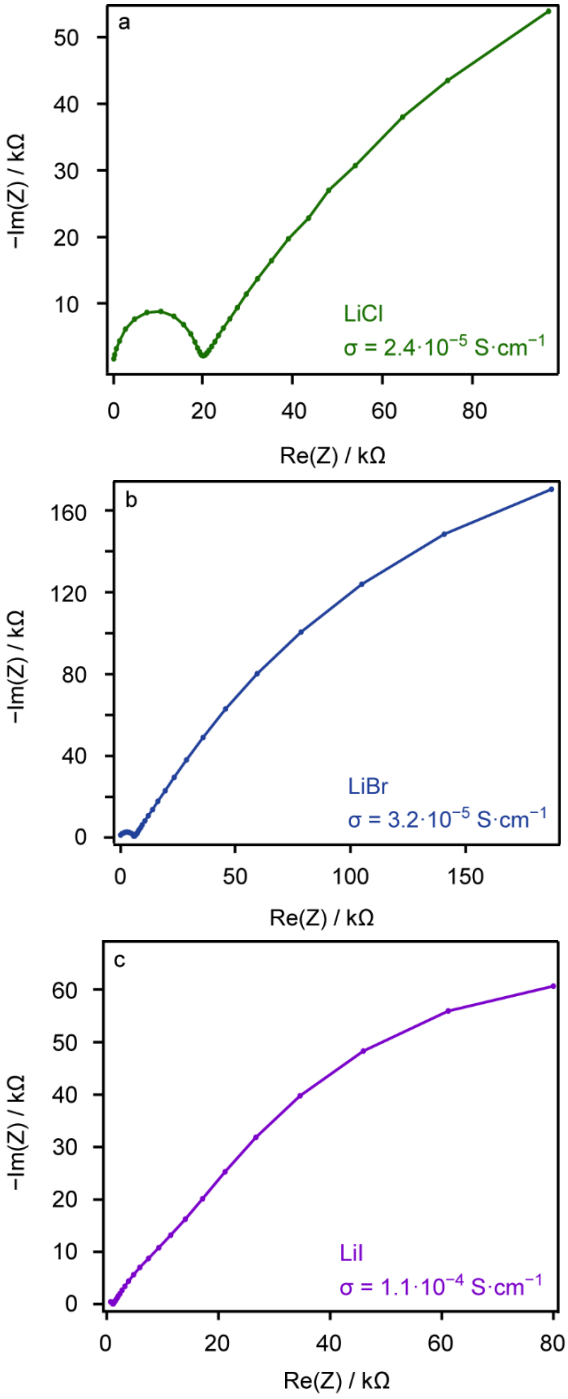

Figure 2. Electrochemical impedance spectra of MOF-LiCl (green, a), MOF-LiBr (blue, b), and MOF-LiI (purple, c), and corresponding conductivity values, collected at 25 °C.

Table 2. Conductivity, activation energy, and Li^+ transference number values of MOF-Li*X*.

Electrolyte	σ (S·cm⁻¹)	E_a (eV)	Li^+ transference #
MOF-LiCl	$2.4 \cdot 10^{-5}$	0.34	0.69
MOF-LiBr	$3.2 \cdot 10^{-5}$	0.30	0.42
MOF-LiI	$1.1 \cdot 10^{-4}$	0.24	0.34

activation energies of < 0.4 eV are on-par with those of superionic conductors.[30]

Li^+ transference numbers for MOF-*LiX*. To evaluate the contribution of Li^+ ions to the ionic current, Li^+ transference numbers were calculated for MOF-Li*X* (Figures S13-S15). MOF-LiCl yielded a high Li^+ transference number of 0.69, indicating that almost 70% of the current passed resulted from mobile Li^+ ions as opposed to other mobile, charged species.[31] This transference number is competitive with many solid electrolytes and a marked improvement upon liquid electrolytes, which typically exhibit Li^+ transference numbers of only 0.3-0.4.[31,32] In the latter, the current is dominated by other mobile ions which can migrate to the electrodes and cause polarization effects that decrease battery lifetime. Ironically, the modularity of the anion identity here produces both quantifiable improvements in terms of conductivity and activation energy of the electrolytes, as well as challenges following these same trends. Thus, Li^+ transference numbers for the MOF-LiBr and MOF-LiI samples were only 0.42 and 0.34, respectively (Table 2). This is likely due to the fact that in addition to ion pairing strength between the Li^+ and the anions decreasing with increasing anion softness, the Coulombic forces immobilizing the anions close to the Cu^{2+} centers also weaken with increasing anion softness.[33] Thus, upon application of electrochemical bias, a higher percentage of Br^- and I^- ions migrate to the opposite electrode compared to Cl^- ions. One possible solution could involve utilizing anions of enhanced steric bulk so that their mobility is more limited compared to those of monoatomic anions. A caveat with this approach may be that significantly increasing the anion size could result in lower loading of the desired metal salt, due to pore volume constraints within the MOF.

Durability studies with MOF-*LiX*. Electrochemical cycling experiments revealed good durability for the MOF-Li*X* electrolytes. Over 200 cycles, MOF-LiCl and MOF-LiBr retained reversible stripping and plating of Li, with only slight increase in overpotential (Figure S16). Additionally, the crystallinity of the structures was retained during extended electrochemical measurements (Figure S8). Interestingly, MOF-LiCl showed an increase in anodic current between cycles 1 and 30, after which time the current then decreased with progressing cycles. This may be due to slower kinetics observed in MOF-LiCl, consistent with the lower conductivity compared to that of MOF-LiBr. MOF-LiBr passed the maximum faradaic current during the first cycle, and current decreased over subsequent cycles. As expected, these cycling measurements also highlighted the instability of MOF-LiI, which lost all faradaic current after only 78 cycles.

As another measure of robustness, the MOF-Li*X* electrolytes showed large potential stability windows. In particular, MOF-LiCl exhibits a potential window of 4.5 V, potentially suitable for battery applications.[34] MOF-LiBr features a slightly narrower potential window of 3.5 V, likely due to partial oxidation of Br^- (Figure S17). Both MOF-LiCl and MOF-LiBr possess potential windows wider than those of many non-aqueous liquid electrolytes, which are commonly limited to ~3 V.[35]

Mg^{2+} transport studies. Although the high volumetric capacity and reversible redox activity intrinsic to lithium identifies Li and Li-ion batteries as attractive energy sources, safety, performance, and abundance (consequently, cost) obstacles that cannot be overcome with cell optimization has encouraged exploration of other metals for battery applications. Mg^{2+}, although less reducing than Li^+, has almost double the volumetric capacity of Li^+, due to its divalent charge and still relatively small ionic radius.[2] Additionally, Mg is not plagued by the dendrite formation issues faced by Li, and is 5 orders of magnitude more abundant than Li.[2] As such, we sought to explore the potential of $Cu_4(ttpm)_2 \cdot 0.6CuCl_2$ as a solid electrolyte for Mg^{2+}. EIS of MOF-$MgCl_2$ and MOF-$MgBr_2$ collected at 25 °C revealed the same modular trend as observed in the Li^+ analogues, in that the bromide salts lead to higher conductivity than chloride (Figure 3, Table 3). Most importantly, MOF-$MgBr_2$ exhibits an ionic conductivity of $1.3 \cdot 10^{-4}$ S·cm⁻¹, and thus shares the spotlight as the most conductive Mg^{2+}-ion solid electrolyte to date.[21] Activation energies calculated from the temperature-dependent EIS data fit to Arrhenius plots were in-line with the trend observed for Li^+ salts: the values were

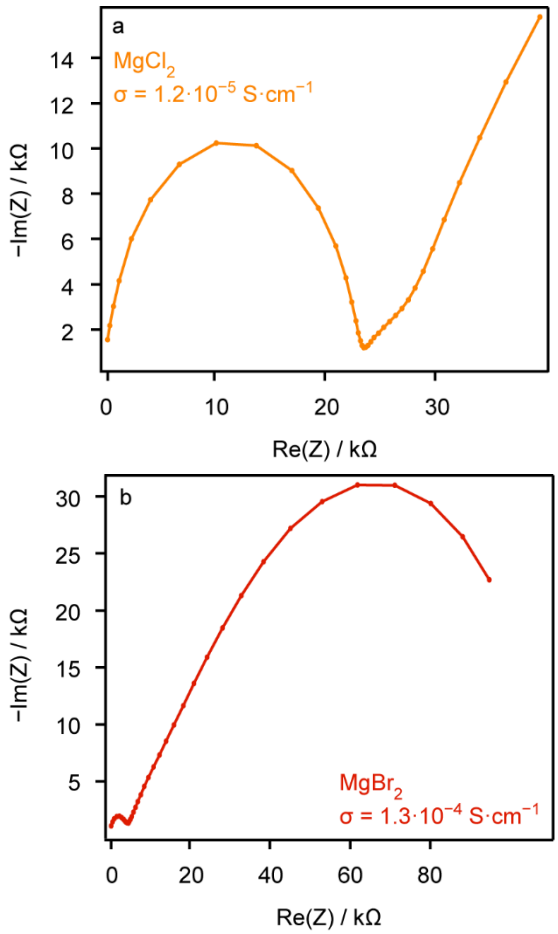

Figure 3. Electrochemical impedance spectra of MOF-$MgCl_2$ (orange, a) and MOF-$MgBr_2$ (red, b), and corresponding conductivity values, collected at 25 °C.

0.32 eV for MOF-$MgCl_2$ and 0.24 eV for MOF-$MgBr_2$ (Figures 4, S18, and Table 3). This data serves as an exciting foundation for further exploring the potential of MOFs as solid electrolytes for high-valent ions such as Mg^{2+}.

Table 3. Conductivity and activation energy values of MOF-MgX_2.

Electrolyte	σ (S·cm^{-1})	E_a (eV)
MOF-$MgCl_2$	$1.2\cdot10^{-5}$	0.32
MOF-$MgBr_2$	$1.3\cdot10^{-4}$	0.24

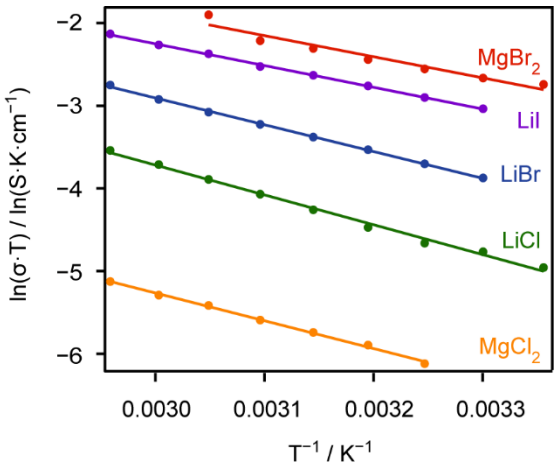

Figure 4. Arrhenius plots for the respective MOF-MX_n electrolytes, used to calculate the activation energy values. MOF-$MgBr_2$ shows the highest conductivity out of all analogues tested, and is among the most conductive solid Mg^{2+} electrolytes reported.

Al^{3+} transport studies. Indeed, encouraged by the results obtained with Mg^{2+}, we also explored the performance of $Cu_4(ttpm)_2\cdot0.6CuCl_2$ as host for Al^{3+}, another attractive member of high-valent batteries.[36] Measuring the ionic conductivity of $Cu_4(ttpm)_2(CuCl_2)_{0.6}(AlCl_3)_{0.5}\cdot20PC$ (MOF-$AlCl_3$), an electrolyte accessed by soaking the MOF in a THF solution of anhydrous $AlCl_3$, gave an average conductivity value of $8.1\cdot10^{-6}$ S·cm^{-1} at 25 °C and an activation energy of 0.32 eV (Figures S19, S20). As with LiCl and $MgCl_2$, MOF-$AlCl_3$ remains crystalline during electrochemical measurements (Figure S21). Although the measured conductivity values fall several orders of magnitude below previously reported solid and liquid Al^{3+} electrolytes,[36,37] these experiments confirm the ability of MOFs to serve as hosts for higher-valent ions.

CONCLUSION

These results demonstrate that a high density of Li^+, Mg^{2+}, and Al^{3+} can be loaded in a Cu-azolate MOF featuring an abundance of open metal sites that bind stoichiometric amounts of halides. Ionic conductivity traces with the softness of the halide ions. Less predictably, the halide-loaded MOFs exhibit modest conductivity for Al^{3+} and record conductivity for Mg^{2+} when compared to other classes of solid electrolytes, with good, but not record conductivity for Li^+. These observations point to a potential connection between pore size, pore polarity, and mobile ion identity that combine better for promoting Mg^{2+}-ion transport in $Cu_4(ttpm)_2\cdot0.6CuCl_2$ than in other materials. Indeed, there may be an ideal pore size and pore polarity that will minimize activation energy for these higher valence ions. Owing to their compositional and structural tunability, MOFs are attractive targets for exploring this possibility.

ASSOCIATED CONTENT

Supporting Information. Materials and Methods. Weight percentages of M^{n+} ions in the electrolytes. ^{1}H NMR spectra of MOF-MX_n/PC. [110] reflection of $Cu[(Cu_4Cl)(ttpm)_2]_2\cdot CuCl_2$. Electrolyte potential windows of MOF-LiX. SEM-EDS. I-V curve of $Cu_4(ttpm)_2\cdot0.6CuCl_2$. Variable temperature EIS spectra of MOF-MX_n. Li^+ transference number data of MOF-LiX. Li redox CVs with MOF-LiX. Arrhenius data of MOF-$AlCl_3$.

The Supporting Information is available free of charge on the ACS Publications website.

AUTHOR INFORMATION

Corresponding Author

mdinca@mit.edu

Notes

The authors declare no competing financial interests.

ACKNOWLEDGMENT

This work was supported by the U.S. Department of Energy, Office of Science, Office of Basic Energy Sciences (DE-SC0018235). E.M.M. gratefully acknowledges the National Science Foundation for partial support through a Graduate Research Fellowship under Grant No. 1122374.

REFERENCES

(1) Kurzweil, P. Gaston Planté and his invention of the lead–acid battery—the genesis of the first practical rechargeable battery. *J. Power Sources* **2010**, *195*, 4424–4434.

(2) Bucur, C. B. *Challenges of a Rechargeable Magnesium Battery*; SpringerBriefs in Energy; Springer International Publishing: Cham, 2018.

(3) Zhao, C.; Liu, L.; Qi, X.; Lu, Y.; Wu, F.; Zhao, J.; Yu, Y.; Hu, Y.; Chen, L. Solid-state sodium batteries. *Adv. Energy Mater.* **2018**, *8*, 1703012-1703031.

(4) Sun, C.; Liu, J.; Gong, Y.; Wilkinson, D. P.; Zhang, J. Recent advances in all-solid-state rechargeable lithium batteries. *Nano Energy* **2017**, *33*, 363–386.

(5) Ngai, K. S.; Ramesh, S.; Ramesh, K.; Juan, J. C. A review of polymer electrolytes: fundamental, approaches and applications. *Ionics* **2016**, *22*, 1259–1279.

(6) Zhao, Y.; Daemen, L. L. Superionic conductivity in lithium-rich anti-perovskites. *J. Am. Chem. Soc.* **2012**, *134*, 15042–15047.

(7) Li, S.; Zhu, J.; Wang, Y.; Howard, J. W.; Lü, X.; Li, Y.; Kumar, R. S.; Wang, L.; Daemen, L. L.; Zhao, Y. Reaction mechanism studies towards effective fabrication of lithium-rich anti-perovskites Li_3OX (X = Cl, Br). *Solid State Ionics* **2016**, *284*, 14–19.

(8) Wang, Y.; Wang, Q.; Liu, Z.; Zhou, Z.; Li, S.; Zhu, J.; Zou, R.; Wang, Y.; Lin, J.; Zhao, Y. Structural manipulation

approaches towards enhanced sodium ionic conductivity in Na-rich antiperovskites. *J. Power Sources* **2015**, *293*, 735–740.

(9) Tang, W. S.; Matsuo, M.; Wu, H.; Stavila, V.; Zhou, W.; Talin, A. A.; Soloninin, A. V.; Skoryunov, R. V.; Babanova, O. A.; Skripov, A. V.; Unemoto, A; Orimo, S.; Udovic, T. Liquid-like ionic conduction in solid lithium and sodium monocarba-closo-decaborates near or at room temperature. *Adv. Energy Mater.* **2016**, *6*, 1502237-1502242.

(10) Hayashi, A.; Nishio, Y.; Kitaura, H.; Tatsumisago, M. Novel technique to form electrode–electrolyte nanointerface in all-solid-state rechargeable lithium batteries. *Electrochem. Commun.* **2008**, *10*, 1860–1863.

(11) Kitaura, H.; Hayashi, A.; Ohtomo, T.; Hama, S.; Tatsumisago, M. Fabrication of electrode–electrolyte interfaces in all-solid-state rechargeable lithium batteries by using a supercooled liquid state of the glassy electrolytes. *J. Mater. Chem.* **2011**, *21*, 118–124.

(12) Ohta, N.; Takada, K.; Sakaguchi, I.; Zhang, L.; Ma, R.; Fukuda, K.; Osada, M.; Sasaki, T. $LiNbO_3$-coated $LiCoO_2$ as cathode material for all solid-state lithium secondary batteries. *Electrochem. Commun.* **2007**, *9*, 1486–1490.

(13) Ohta, N.; Takada, K.; Zhang, L.; Ma, R.; Osada, M.; Sasaki, T. Enhancement of the high-rate capability of solid-state lithium batteries by nanoscale interfacial modification. *Adv. Mater.* **2006**, *18*, 2226–2229.

(14) Takada, K.; Ohta, N.; Zhang, L.; Fukuda, K.; Sakaguchi, I.; Ma, R.; Osada, M.; Sasaki, T. Interfacial modification for high-power solid-state lithium batteries. *Solid State Ionics* **2008**, *179*, 1333–1337.

(15) Sakuda, A.; Kitaura, H.; Hayashi, A.; Tadanaga, K.; Tatsumisago, M. Improvement of high-rate performance of all-solid-state lithium secondary batteries using $LiCoO_2$ coated with Li_2O–SiO_2 glasses. *Electrochem. Solid-State Lett.* **2008**, *11*, A1-A3.

(16) Sakuda, A.; Kitaura, H.; Hayashi, A.; Tadanaga, K.; Tatsumisago, M. Modification of interface between $LiCoO_2$ electrode and Li_2S–P_2S_5 solid electrolyte using Li_2O–SiO_2 glassy layers. *J. Electrochem. Soc.* **2009**, *156*, A27-A32.

(17) Woo, J. H.; Trevey, J. E.; Cavanagh, A. S.; Choi, Y. S.; Kim, S. C.; George, S. M.; Oh, K. H.; Lee, S. Nanoscale interface modification of $LiCoO_2$ by Al_2O_3 atomic layer deposition for solid-state Li batteries. *J. Electrochem. Soc.* **2012**, *159*, A1120–A1124.

(18) Park, S. S.; Tulchinsky, Y.; Dincă, M. Single-ion Li^+, Na^+, and Mg^{2+} solid electrolytes supported by a mesoporous anionic Cu–azolate metal–organic framework. *J. Am. Chem. Soc.* **2017**, *139*, 13260–13263.

(19) Wiers, B. M.; Foo, M.; Balsara, N. P.; Long, J. R. A solid lithium electrolyte via addition of lithium isopropoxide to a metal–organic framework with open metal sites. *J. Am. Chem. Soc.* **2011**, *133*, 14522–14525.

(20) Ameloot, R.; Aubrey, M.; Wiers, B. M.; Gómora-Figueroa, A. P.; Patel, S. N.; Balsara, N. P.; Long, J. R. Ionic conductivity in the metal-organic framework UiO-66 by dehydration and insertion of lithium tert-butoxide. *Chem. Eur. J.* **2013**, *19*, 5533–5536.

(21) Aubrey, M. L.; Ameloot, R.; Wiers, B. M.; Long, J. R. Metal–organic frameworks as solid magnesium electrolytes. *Energy Environ. Sci.* **2014**, *7*, 667-671.

(22) Shen, L.; Wu, H. Bin; Liu, F.; Brosmer, J. L.; Shen, G.; Wang, X.; Zink, J. I.; Xiao, Q.; Cai, M.; Wang, G.; Lu, Y.; Dunn, B. Creating lithium-ion electrolytes with biomimetic ionic channels in metal-organic frameworks. *Adv. Mater.* **2018**, *30*, 1707476-1707483.

(23) Cepeda, J.; Pérez-Yáñez, S.; Beobide, G.; Castillo, O.; Goikolea, E.; Aguesse, F.; Garrido, L.; Luque, A.; Wright, P. A. Scandium/alkaline metal–organic frameworks: Adsorptive properties and ionic conductivity. *Chem. Mater.* **2016**, *28*, 2519–2528.

(24) Dincă, M.; Dailly, A.; Long, J. R. Structure and charge control in metal-organic frameworks based on the tetrahedral ligand tetrakis(4-tetrazolylphenyl)methane. *Chem. Eur. J.* **2008**, *14*, 10280–10285.

(25) Traube, I. Ueber kupferjodid. *Deutsch. Chem. Ges.* **1884**, *17*, 1064-1067.

(26) Kolthoff, I. M. The reaction between cupric copper and iodide and between cuprous iodide and iodine. *Recl. des Trav. Chim. des Pays-Bas.* **1926**, *45*, 153–161.

(27) Holleman, A. F.; Wiberg, E. *Inorganic Chemistry*; Academic Press: San Diego, 2001.

(28) Copper, Silver and Gold. In *Chemistry of the Elements*; Greenwood, N. N., Earnshaw, A., Eds.; Elsevier, 1997, 1173–1200.

(29) Goodenough, J. B.; Kim, Y. Challenges for rechargeable Li batteries. *Chem. Mater.* **2010**, *22*, 587–603.

(30) Linford, R. G.; Hackwood, S. Physical techniques for the study of solid electrolytes. *Chem. Rev.* **1981**, *81*, 327–364.

(31) Zugmann, S.; Fleischmann, M.; Amereller, M.; Gschwind, R. M.; Wiemhöfer, H. D.; Gores, H. J. Measurement of transference numbers for lithium ion electrolytes via four different methods, a comparative study. *Electrochim. Acta* **2011**, *56*, 3926–3933.

(32) Diederichsen, K. M.; McShane, E. J.; McCloskey, B. D. Promising routes to a high Li^+ transference number electrolyte for lithium ion batteries. *ACS Energy Lett.* **2017**, *2*, 2563–2575.

(33) *CRC Handbook of Chemistry and Physics*, 81st ed.; Lide, D. R., Ed.; CRC Press: Boca Raton, 2000.

(34) Wang, L.; Chen, B.; Ma, J.; Cui, G.; Chen, L. Reviving lithium cobalt oxide-based lithium secondary batteries-toward a higher energy density. *Chem. Soc. Rev.* **2018**, *47*, 6505–6602.

(35) Goodenough, J. B.; Park, K. The Li-ion rechargeable battery: A perspective. *J. Am. Chem. Soc.* **2013**, *135*, 1167–1176.

(36) Zhang, Y.; Liu, S.; Ji, Y.; Ma, J.; Yu, H. Emerging nonaqueous aluminum-ion batteries: Challenges, status, and perspectives. *Adv. Mater.* **2018**, *30*, 1706310-1706334.

(37) Schoetz, T.; de Leon, C. P.; Ueda, M.; Bund, A. Perspective—state of the art of rechargeable aluminum batteries in non-aqueous systems. *J. Electrochem. Soc.* **2017**, *164*, A3499–A3502.

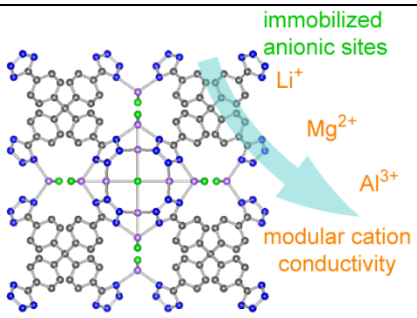
immobilized
anionic sites
Li+
Mg2+
Al3+
modular cation
conductivity